BMC Molecular and Cell Biology

RESEARCH

Open Access

Role of layilin in regulating mitochondria-mediated apoptosis: a study on B cell lymphoma (BCL)-2 family proteins

Mitsumi Arito[1*], Atsuhiro Tsutiya[1], Masaaki Sato[1], Kazuki Omoteyama[1], Toshiyuki Sato[1], Yusei Motonaga[1], Naoya Suematsu[1], Manae S. Kurokawa[2] and Tomohiro Kato[1]

Abstract

Background Malignant gliomas exhibit rapid tumor progression and resistance to treatment, leading to high lethality. One of the causes is the reduced progression of apoptosis in glioma cells. Layilin is a type 1 transmembrane protein with a C-type lectin motif in its extracellular domain. We previously reported that layilin is mainly localized to mitochondria or their close proximity and that layilin is essential for maintaining of the fragmented type of mitochondria. This study investigates the effects of layilin on mitochondria-mediated apoptosis, focusing on B cell lymphoma (BCL)-2 family proteins in a glioma cell line of A172 cells.

Results We compared the levels of pro-apoptotic BCL-2 family proteins of BAD, BAK, BAX, and BIM and anti-apoptotic BCL-2 family proteins of BCL-2 and BCL-X_L between layilin- knockdown (KD) cells and control cells using western blot. The protein levels of BAD were significantly smaller in layilin-KD cells than in control cells, while those of BCL-2 were significantly larger. We then compared the mitochondrial membrane potential (ΔΨm) under p-trifluoromethoxyphenyl hydrazone (FCCP)-treated conditions using MT-1 staining. In layilin-KD cells, ΔΨm was significantly larger and FCCP-induced ΔΨm reduction was significantly lower than in control cells. Furthermore, we examined the levels of cell membrane-bound Annexin V and DNA-bound propidium idodide (PI) in layilin-KD cells with/without staurosporine (STS) treatment. Layilin-KD significantly decreased levels of cell membrane-bound Annexin V with/without STS treatment. On the other hand, PI levels were not changed by layilin-KD. We also investigated the amounts of the active caspase (CASP)-3, CASP-6, CASP-7, and poly (ADP-ribose) polymerase-1 (PARP1, cleaved form), as well as DNA fragmentation in layilin-KD cells under apoptotic conditions induced by STS, using western blot and the DNA ladder method, respectively. Under STS-treated conditions, the amounts of active CASP-3, CASP-7, and poly (ADP-ribose) PARP1 were significantly smaller in layilin-KD cells than in control cells. Accordingly, DNA fragmentation was significantly suppressed in layilin-KD cells compared to control cells under STS-treated conditions.

Conclusion This study demonstrates that layilin contributes to ΔΨm reduction to promote apoptosis by up-regulating BAD and down-regulating BCL-2 in glioma cells. Our data elucidates a new function of layilin: regulation of mitochondria-mediated apoptosis.

*Correspondence:
Mitsumi Arito
m-ari@marianna-u.ac.jp

Full list of author information is available at the end of the article

Keywords Apoptosis, BAD, BCL-2, Layilin

Background

Gliomas account for 25–30% of brain tumors and arise from glial cells, which support brain neuronal cells in the central nervous system [1]. Malignant gliomas (World Health Organization grades III and IV) exhibit rapid tumor progression and resistance to treatment, leading to high lethality [2, 3]. One of the causes of this is the reduced progression of apoptosis in glioma cells [4].

Layilin is a type 1 transmembrane protein known for containing a C-type lectin motif in its extracellular domain [5]. It has been reported to function as a hyaluronic acid receptor [6]. Previous studies have indicated interactions between layilin and cytoskeletal proteins including talin, merlin, and radixin [5, 7]. Layilin has been observed along the leading edge of migrating cells [5], and on the surface of immune cells [8], suggesting potential roles near or at the cell membrane. However, our previous research has demonstrated that layilin is primarily localized in the cytoplasm rather than on the cell surface [9]. Furthermore, we have reported that layilin is predominantly found in mitochondria or in close proximity to them, and it plays a crucial role in maintaining the fragmented type of mitochondria [10].

Mitochondria are well known for their role in ATP production through oxidative phosphorylation. More recently, their involvement in cellular apoptosis has been highlighted. In response to apoptotic stimuli, the mitochondrial membrane potential ($\Delta\Psi m$) decreases, accompanied by the release of cytochrome C from mitochondria, which activates the apoptosis process [11–13]. From the perspective of mitochondrial morphology, mitochondrial fission is increased during the induction of apoptosis [14]. In general, elongated mitochondria tend to show a high membrane potential, while fragmented mitochondria tend to show a low membrane potential [14, 15]. Thus, the condition and morphology of mitochondria is crucial for apoptosis.

The B cell lymphoma (BCL)-2 family proteins play a significant role in regulating mitochondrial outer membrane permeability and, therefore, apoptosis control [16, 17]. Among these proteins, BCL-2 associated agonist of cell death (BAD), BCL-2 antagonist/killer 1 (BAK), BCL-2 associated X (BAX), and BCL-2 interacting mediator of cell death (BIM) are known for their pro-apoptotic functions, while BCL-2 and BCL-X_L have anti-apoptotic functions [16, 17]. Upon exposure to apoptotic stimuli, cytoplasmic BAX translocates to mitochondria, forming BAX/BAK pores across the mitochondrial outer membrane. These pores allow the release of mitochondrial cytochrome C into the cytosol [18, 19]. BAK and BAX have also been shown to promote the mitochondrial permeability transition pore (mPTP) formation, which contributes to the release of cytochrome C into the cytosol [20]. Released cytochrome C is known to form the apoptosome with apoptotic peptidase activating factor 1 and CASP-9, thus activating the caspase signaling cascade [21, 22]. Specifically, the activated cleaved form of CASP-9 triggers the activation of effector caspases such as CASP-3, CASP-6, and CASP-7. These active cleaved effector caspases further activate downstream proteins like poly (ADP-ribose) polymerase-1 (PARP1) and Lamin-A/B1/B2, ultimately leading to apoptosis [21, 22]. Conversely, BCL-2 and BCL-X_L on the mitochondrial outer membrane directly inhibit mPTP function and/or BAX/BAK pore formation by binding to BAX [17, 20, 23]. This process suppresses cytochrome C-mediated caspase cascade activation [17, 20, 23]. Additionally, BAD as well as BIM, forming a dimer with BCL-2 and with BCL-X_L (BAD/BCL-2, BAD/BCL-X_L, BIM/BCL-2, and BIM/BCL-X_L dimers), reduce the activity of BCL-2 and BCL-X_L [24, 25]. This promotes the activation of the BAX/BAK-mediated caspase cascade [24, 25].

It is reported that layilin helps maintain mitochondrial fission and that mitochondrial fission increases during apoptosis [14], layilin possibly plays a role in the early stages of apoptosis. Thus, our study aimed to investigate the effects of layilin on mitochondria-mediated apoptosis, with a specific focus on the BCL-2 family proteins in glioma cells.

Methods

Cell culture

A172 cells, a human malignant glioma cell line (DS Pharma Biomedical Co., LTD, Osaka, Japan) were grown in an RPMI-1640 medium (Sigma-Aldrich, St. Louis, MO, USA). The culture medium was supplemented with 10% fetal bovine serum (FBS), 100 units/ml penicillin, and 100 μg/ml streptomycin (Sigma-Aldrich). The cells were cultured at 37 °C and in a humidified atmosphere with 5% CO_2.

Immunocytochemistry

A172 cells were cultured on ϕ35 mm type I collagen-coated glass bottom dishes (AGC Techno Glass Co., Ltd., Shizuoka, Japan) and fixed with 4% paraformaldehyde in phosphate buffered saline (PBS) for 15 min. Next, cells were washed with PBS, permeabilized with PBS plus 0.3% TritonX for 10 min, and blocked with PBS plus 5% bovine serum albumin for 1 h at room temperature. Cells were then reacted with primary antibodies overnight at 4 °C. The primary antibodies used were anti-TOMM20 (1:200, D8T4N, Cell Signaling Technology Inc. (CST))

and anti-layilin (1:100, C7, Santa Cruz, Dallas, TX, USA). The cells, washed with PBS, were then reacted with goat anti-mouse IgG antibodies labeled with AlexaFluor488 (Invitrogen, Carlsbad, CA, USA) and goat anti-rabbit IgG antibodies labeled with AlexaFluor 568 (Invitrogen) for 1 h at room temperature. Finally, cells were stained with DAPI and coverslips were applied using ProLong Glass antifade mountant (Invitrogen). Super-resolution images of the cells were obtained by LSM900 Airyscan super-resolution system (Carl Zeiss, Jena, Germany). Z-stack images were obtained at 0.19 μm intervals. To analyze the colocalization of layilin and TOMM20, we employed orthogonal projections with Fiji software [26].

RNA interference

A172 cells were transfected with 200 pmol of siRNA per 100 mm dish using Lipofectamine RNAiMAX (Invitrogen). Two different siRNA sequence were employed to target human layilin mRNA: siL1 (nucleotides 1019–1043, AAGCUGCCUUGAAUCUGGCCUACAU) and siL2 (nucleotides 1564–1588, CACAGAAGGUCUAU GAACAAGCUUA) based on NM_001258390.1 (Invitrogen). As a negative control, A172 cells were similarly transfected with a control siRNA (siC, Stealth™ RNAi Negative Control Medium GC Duplex, Invitrogen).

Western blotting

The cultured A172 cells, collected and washed with PBS, were sonicated in a lysis buffer composed of 20 mM Tris-HCl, 250 mM NaCl, 1% NP-40, 1 mM dithiothreitol, and a protease inhibitor cocktail (Roche, Basel, Switzerland). Following centrifugation, the supernatants were used as whole-cell protein samples. Western blotting was conducted as previously described [9]. The protein samples, separated using 15% sodium dodecyl sulfate-polyacrylamide gel electrophoresis, were subsequently transferred onto polyvinylidence difluoride membranes. Goat polyclonal antibodies against human layilin (R&D Systems Inc., Minneapolis, MN, USA), mouse monoclonal antibodies against human BAD (SantaCruz, Dallas, TX, USA), BAK (SantaCruz), BAX (SantaCruz), BIM (SantaCruz), BCL-2 (SantaCruz), BCL-X_L, (SantaCruz), and β-actin (Sigma) were used as primary antibodies. Additionally, rabbit monoclonal antibodies against human cleaved CASP-3 (abcam, Cambridge, UK), PARP1 (abcam), and CASP-7 (CST, Danvers, MA, USA), as well as rabbit polyclonal antibodies against human cleaved CASP-6 (CST) were used as primary antibodies. Horseradish peroxidase (HRP)-conjugated rabbit anti-goat IgG antibodies (Agilent/DAKO, Santa Clara, CA, USA), anti-mouse IgG antibodies (CST), and anti-rabbit IgG antibodies (CST) were used as secondary antibodies. The bound antibodies were visualized using ImmunoStar® LD (Fuji Film, Osaka, Japan).

RNA extraction, reverse transcription, and quantitative PCR (qPCR)

RNA extraction and RT-PCR were conducted as previously outlined [27]. To summarize, RNA extraction and purification from A172 cells, as well as reverse transcription of the RNA samples, were carried out using RNeasy (Qiagen, Venlo, The Netherlands) and High-Capacity cDNA Reverse Transcription Kits (Life Technologies, Rockville, MD, USA), respectively, following the manufacturer's instructions. qPCR was performed using the ABI Prism 7000 Sequence Detection System (Applied Biosystems, Foster city, CA, USA). To measure mRNA levels for layilin and glyceraldehyde 3-phosphate dehydrogenase (GAPDH), a mixture containing 2 μg of total RNA-derived cDNA, 300 nM of each forward and reverse primer, and Power SYBR® Master Mix (Applied Biosystems) was subjected to qPCR. The nucleotide sequences of the primers are as follows: layilin: 5'-CAC AGCCTGCCAGGACCTTTA and 5'-TGCACCGGTCA TCATTCCA, while GAPDH: 5'-TGGTATGGTGGAAG GACTCA and 5'-ATGCCAGTGAGCTTCCCGTT. For the measurement of mRNA for BAD and BCL-2, a mixture of 2 μg of total RNA-derived cDNA, a solution of TaqMan® Gene Expression Assays (Hs00188930_m1 and Hs04986394_s1, respectively, Applied Biosystems), and TaqMan® Gene Expression Master Mix (Applied Biosystems) were subjected to qPCR. The thermal cycling conditions were as follows: 95 °C for 10 min, followed by 40 cycles of 95 °C for 15 s and 60 °C for 60 s.

Assessment of mitochondrial membrane potential MT-1 staining

The fluorescent dye MT-1 used in this study is a cell-permeable cation that selectively accumulates in mitochondria in the presence of a ΔΨm gradient. Therefore, recently, dyes of this class are commonly used to assess ΔΨm, similarly to TMRE and JC-1 [28, 29]. Specifically, mitochondrial membrane potential was assessed using MT-1 MitoMP Detection Kit (DOJINDO LABORATORIES, Kumamoto, Japan), according to the manufacturer's instructions. A172 cells, which had been transfected with siL-1, siL-2 or siC (8.0×10^4 cells) in RPMI containing 10% FBS, were seeded onto 35 mm glass-based dishes (ASAHI GLASS, Tokyo, Japan). After a 24 h incubation, the culture medium was replaced with serum-free RPMI containing MT-1. Following a 30 min incubation, the cells were washed with Hanks' balanced salt solution (HBSS) and expose to serum-free RPMI containing 5 μM carbonyl cyanide p-trifluoromethoxyphenyl hydrazone (FCCP) of a protonophore for 30 min. Subsequently, the cells were washed with HBSS and fixed in PBS containing 4% paraformaldehyde. The MT-1 signal was visualized using a fluorescence microscope (BIOREVO (BZ-9000), KEYENCE, Jena, Germany). The

fluorescence intensity of MT-1 in each pixel was quantified using the BZ-II Analyzer Ver. 1.42 (KEYENCE). The brightness levels were calculated by summing the fluorescence intensity from all the pixels.

Annexin V and propidium idodide (PI) assay

A172 cells, seeded onto a 96 well plate (Corning Inc., Corning, NY, USA), were transfected with siL-1, siL-2 or siC (7.5×10^3 cells) in RPMI containing 10% FBS. After 24 h, the culture medium was replaced RPMI with/without 50 μM STS. Three hours later, cell membrane-bound Annexin V and DNA-bound PI were assessed using RealTime-Glo™ Apoptosis and Necrosis Assay (Promega, Madison, WI, USA) according to the manufacturer's instructions. Cell membrane-bound Annexin V is detected with a luminescence signal, and DNA-bound PI is detected with a fluorescent signal using a microplate reader (Varioskan LUX, Thermo Fisher Scientific Inc., Waltham, MA, USA).

Detection of fragmented DNA

DNA fragmentation was assessed using the ApopLadder Ex™, Apoptotic DNA Fragments Extraction Kit (Takara, Shiga, Japan), following the manufacturer's instructions. Isolated fragmented DNA from cells was then subjected to agarose gel electrophoresis. The DNA within the gels, was made visible through ethidium bromide staining and exposure to ultraviolet light, were photographed, after which photographs were taken.

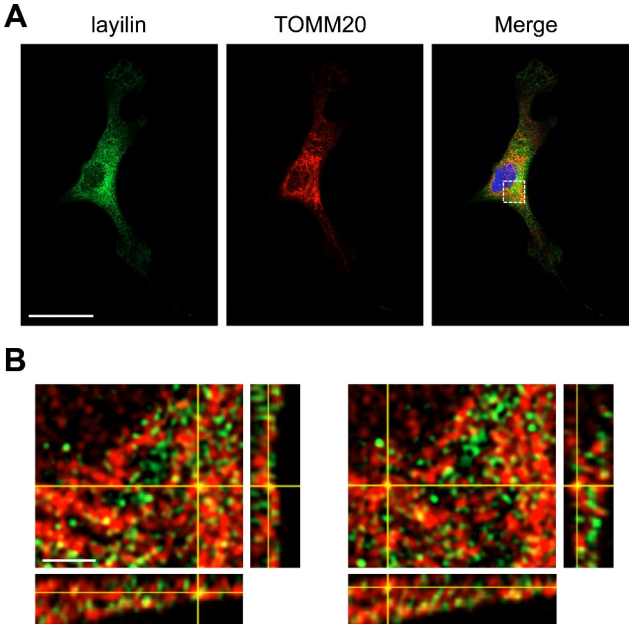

Fig. 1 **(A)** Localization of laylin in A172 cells. Representative super-resolution images were obtained from double immunostaining for layilin (green) and TOMM20 (red) as a mitochondrial marker. Scale bar = 20 μm. **(B)** In the Z-stack analysis, orthogonal projections of the area enclosed by a dotted line in the right panel of Fig. 1 (A) were enlarged. Scale bar = 2 μm

Statistical analysis

Statistical analysis involved using the student's *t*-test and one-way analysis of variance, followed by Tukey's honest significant difference post hoc test for multiple comparisons to determine statistical differences. A significant level of $p<0.05$ was adopted to identify statistically significant results.

Results

A considerable part of layilin localized to mitochondria or in close proximity to them in A172 cells

We have reported that layilin is predominantly found in mitochondria or in close proximity to them in HEK293T cells [6]. To confirm layilin is found in mitochondria or in close proximity to them in A172 cells similarly as HEK293T cells, we investigated co-localization of layilin with a mitochondrial marker, TOMM20 by double immunostaining (Fig. 1A and B). As a result, layilin mainly localized to cytoplasm (Fig. 1A and B). A considerable part of layilin co-localized with TOMM20 not only in 2D images but also in Z-stack images (Fig. 1A and B). These data indicate that layilin localizes to mitochondria or in their close proximity in A172 cells.

Knock-down (KD) of layilin decreased protein levels of BAD, but increased those of BCL-2

Previously, we demonstrated that several malignant glioma cell lines including A172 cells expressed high levels of layilin, compared to astrocytes [9]. Therefore, we here used a knockdown system to assess roles of layilin. To investigate the roles of layilin in the regulation of BCL-2 family proteins, we prepared layilin-KD A172 cells using 2 different siRNAs targeting layilin mRNA (siL1 and siL2). After 24 h of KD, we conducted a western blotting analysis on cell proteins. Firstly, we confirmed that the protein levels of layilin were fully reduced by both siL1 and siL2 (Fig. 2A and B and Additional file 1). Subsequently, we explored the effects of layilin-KD on the levels of pro-apoptotic BCL-2 proteins, including BAD, BAK, BAX, and BIM. We observed a significant decrease in BAD protein levels by nearly half with both siL1 and siL2 (Fig. 2A and C and Additional file 1). However, layilin-KD did not have a significant impact on the levels of BIM and BAK (Fig. 2A and C and Additional file 1). Notably, BAX protein levels were significantly increased by siL-2 but not by siL-1 (Fig. 2A and C and Additional file 1). We also investigated the effects of layilin-KD on the levels of anti-apoptotic BCL-2 proteins, including BCL-2 and BCL-X_L. We found that BCL-2 protein levels were significantly increased by approximately 2-fold with both siL1 and siL2 (Fig. 2A and C and Additional file 1). Protein levels of BCL-X_L showed a tendency to decrease with siL-1 and siL-2 (Fig. 2A and C and Additional file 1). Based on these findings, it was suggested that laylin-KD

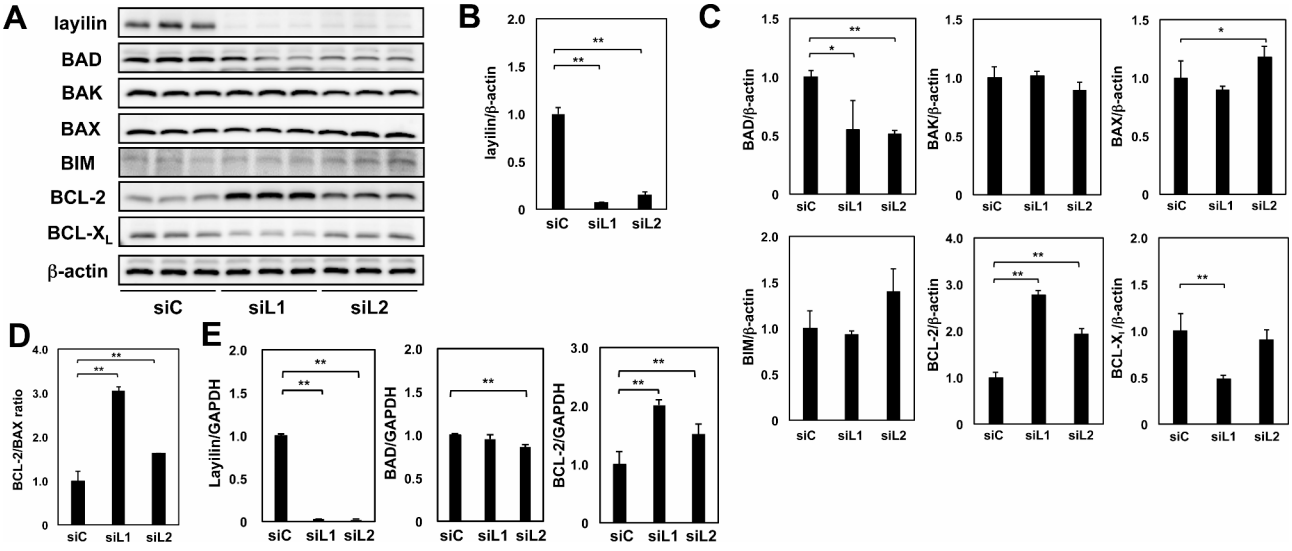

Fig. 2 Effects of laylin-KD on the levels of BCL-2 family proteins in A172 cells. **(A)** A172 cells were transfected with control siRNA (siC) and 2 kinds of layilin siRNA (siL1 and siL2). The protein samples extracted from whole cells underwent western blotting. (**B** and **C**) Band intensities were quantified using densitometry. The intensities of layilin, BAD, BAK, BAX, BIM, BCL-2, and BCL-X_L bands were normalized to β-actin bands. The average normalized intensity in the 'siC' samples set as 1.0. **(D)** The BCL-2/BAX ratios were calculated with the "siC" samples as the reference (defined as 1.0). **(E)** RNA extracted from the cells used for reverse transcription and subject to qPCR to estimate the mRNA levels of layilin, BAD, BCL-2, and GAPDH. Measured mRNA levels of layilin, BAD, and BCL-2 were normalized to GAPDH. In each panel, the average of the normalized or corrected values in siC-transfected samples was defined as 1.0 ($n = 3$ in each condition). Mean values with SD are presented. *$p < 0.05$, ** $p < 0.01$

may specifically regulate at least BCL-2 and BAD in A172 cells. Next, we examined the effects of layilin-KD on BCL-2 and BAD protein levels in U251MG glioma cell line, in addition to A172. The results were consistent with those obtained in A172 cells, which strengthens the possibility that layilin contributes to apoptosis in glioma cell lines (Additional file 2 and 3). The ratio of BCL-2 to BAX (BCL-2/BAX ratio), often used as an anti-apoptotic index, was significantly increased by 1.6-fold or more with siL1 and siL2 (Fig. 2D). These results suggest that layilin either maintains or up-regulates the pro-apoptotic protein BAD and down-regulates the anti-apoptotic protein BCL-2. In light of these findings, layilin is implicated in promoting apoptosis.

Moving forward, we assessed the impact of layilin-KD on mRNA levels of BAX and BCL-2. We confirmed that the expression of layilin mRNA was fully suppressed by both siRNAs (Fig. 2E). Subsequently, we found that mRNA levels for BAD were significantly decreased by siL-2 and exhibited a decreasing trend with siL-1. Conversely, mRNA levels for BCL-2 were significantly increased by both siL1 and siL2. (Fig. 2E). These findings indicate that layilin up-regulates BCL-2 mRNA levels, consistent with the increased BCL-2 protein levels described as above.

Layilin-KD increased the ΔΨm and suppressed FCCP-induced ΔΨm reduction

Given that a reduction in ΔΨm is a response to apoptotic stimuli, we investigated impact of layilin-KD on ΔΨm using MT-1 staining (Fig. 3A). Under non-treated condition (FCCP (-)), we observed a significant increase in ΔΨm in siL1-transfected cells and a tendency for an increase in siL2-transfected cells when compared to siC-transfected cells (Fig. 3B, closed bars). In siC-transfected cells, treatment with FCCP resulted in a significant ~ 30% reduction in ΔΨm (Fig. 3B, closed vs. open bars). However, in siL1- and siL2- transfected cells, the reduction in ΔΨm due to FCCP treatment was only 10%. Consequently, in the presence of FCCP, a statistically significant increase of approximately 50% in ΔΨm was observed in siL1- and siL2-transfected cells compared to siC-transfected cells (Fig. 3B, open bars). These findings indicate that layilin-KD appears to enhance ΔΨm, even under non-apoptotic condition, and significantly suppresses the reduction of ΔΨm during apoptosis. This suggests that layilin plays a role in decreasing ΔΨm.

Layilin-KD suppressed STS-induced apoptosis

To evaluate the impact of layilin-KD on apoptosis, we examined the levels of cell membrane-bound Annexin V and DNA-bound PI in layilin-KD cells with/without STS treatment. As a result, layilin-KD significantly decreased levels of cell membrane-bound Annexin V, and also significantly decreased STS-induced cell membrane-bound Annexin V (Fig. 4A, left). On the other hand, no change in DNA-bound PI was observed in layilin-KD cells with/without STS (Fig. 4A, right). We demonstrated that layilin-KD suppressed apoptosis rather than necrosis. Next, we examined the levels of active apoptosis-related

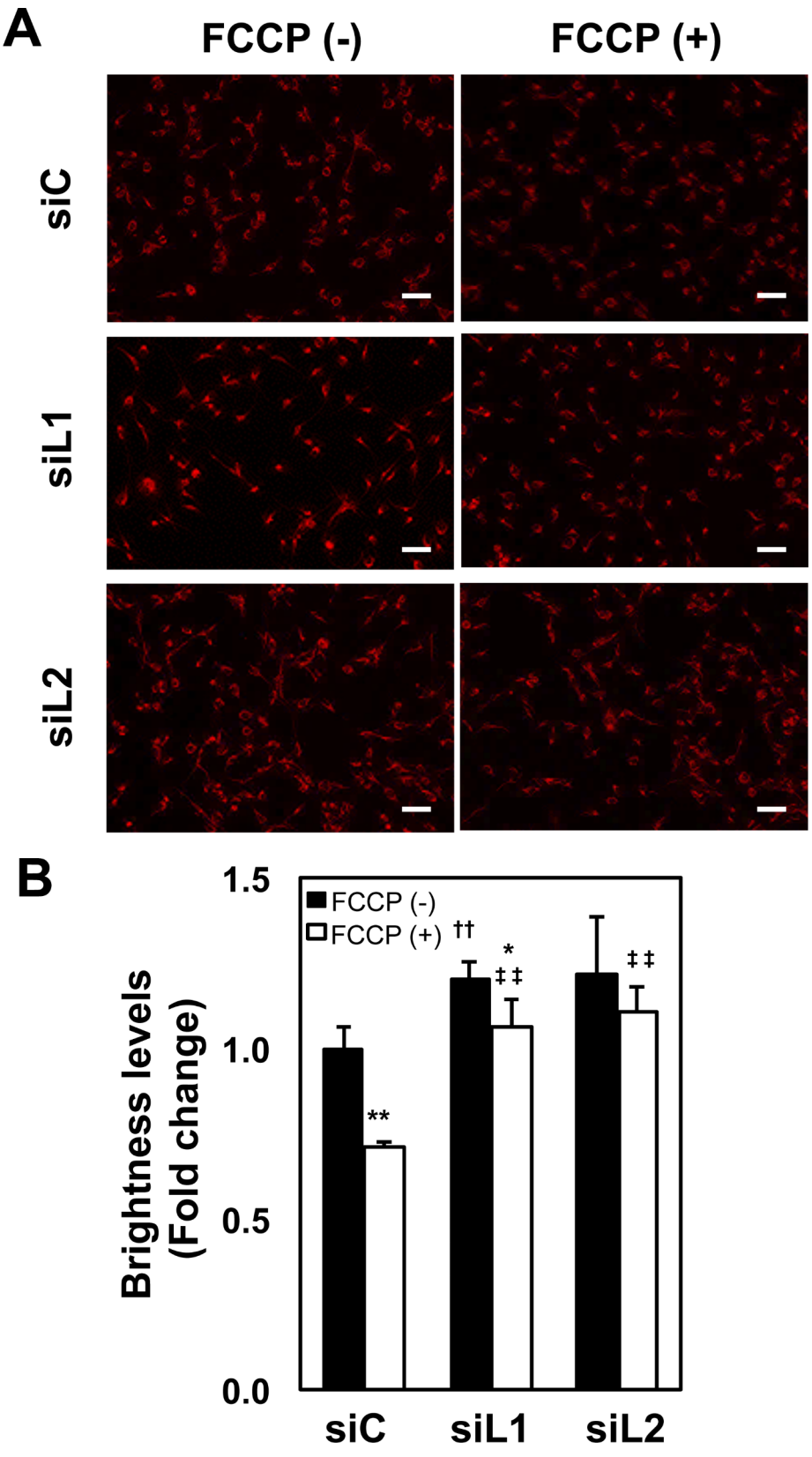

Fig. 3 (See legend on next page.)

(See figure on previous page.)

Fig. 3 Effects of laylin-KD on mitochondrial membrane potential. **(A)** A172 cells, transfected with siL1, siL2 or siC, were plated on 35 mm glass-based dishes. After 24 h, the culture medium was replaced with serum-free RPMI containing MT-1. Following a 30 min incubation, the cells were washed with HBSS, cultured with serum-free RPMI containing 5 μM FCCP for 30 min, and then fixed in PBS containing 4% paraformaldehyde. MT-1 was visualized using a fluorescence microscope. Scale bars: 100 μm. **(B)** The fluorescence intensity of MT-1 was measured using the BZ-II Analyzer Ver. 1.42. Brightness levels were quantified by calculating the sum of fluorescence intensity for all pixels. The average of brightness levels in the 'siC, FCCP (-)' samples, which were transfected with siC, were defined as 1.0 ($n = 3$ in each condition). Mean values with SD are presented. * $p < 0.05$, ** $p < 0.01$ (closed bars vs. open bars), †† $p < 0.01$ (vs. siC, closed bars), ‡‡ $p < 0.01$ (vs. siC, open bars)

proteins of CASP-3, CASP-6, CASP-7, and PARP1 (active form), as well as the presence of fragmented DNA in laylin-KD cells during STS-induced apoptosis. We first verified that the protein levels of laylin were completely suppressed by both siRNAs (Fig. 4B and C and Additional file 4). Subsequently, we observed a substantial increase in the amounts of cleaved apoptosis-related proteins of CASP-3, CASP-6, CASP-7, and PARP1 in cells undergoing apoptosis triggered by STS (Fig. 4B and C and Additional file 4). Moreover, in the STS-treated conditions, laylin-KD cells exhibited significantly smaller amounts of cleaved CASP-3, CASP-7, and PARP1 (by 35–50%) compared to control cells (Fig. 4B and C and Additional file 4). Consequently, the levels of fragmented DNA were also notably reduced in laylin-KD cells, compared to control cells under the STS-induced apoptosis conditions (Fig. 4E). These findings strongly suggest that laylin promotes apoptosis.

Discussion

Our findings can be summarized as follows: (1) Laylin plays a role in maintaining or up-regulating the pro-apoptotic protein of BAD while down-regulating the anti-apoptotic protein of BCL-2. (2) Laylin contributes to decrease of the ΔΨm. (3) Consequently, laylin promotes to apoptosis (Fig. 5).

On the first point, we found that laylin-KD significantly decreased the levels of BAD. BAD is known to reduce the activity of anti-apoptotic proteins such as BCL-2 and BCL-X_L by forming dimers with them (BAD/BCL-2 and BAD/BCL-X_L dimers, respectively) [30]. Consequently, the decrease in BAD due to laylin-KD would result in lower amounts of BAD/BCL-2 and BAD/BCL-X_L dimers. As a result, a relatively larger pool of free BCL-2 and BCL-X_L would be available to form dimers with BAX. Furthermore, we found that laylin-KD significantly increased the protein levels of BCL-2, which would further enhance the formation of BCL-2/BAX dimers. In this context, laylin may increase the levels of BAD, leading to an increase in the formation of BAD/BCL-2 dimers. Additionally, laylin may decrease the levels of BCL-2, leading to a decrease in the formation of BCL-2/BAX dimers (Fig. 5). This reduction in BCL-2/BAX dimers would increase free BAX available to form BAX/BAK dimers in response to apoptotic stimuli (Fig. 5). From this perspective, it appears that laylin promotes the BAX/BAK-mediated caspase cascade (Fig. 5).

Since laylin localizes to mitochondria and their vicinity, it is possible that laylin directly interacts with BCL-2 or BAD. Therefore, we investigated the protein-protein interaction between laylin and BCL-2, as well as between laylin and BAD, using Co-IP. However, direct binding between laylin and BCL-2 or BAD was not evidenced (data not shown). Thereby the regulation is not likely due to direct binding of laylin. On the other hand, BCL-2 mRNA levels significantly increased by laylin-KD, while BAD mRNA levels slightly decreased (Fig. 2E). This suggests that specific regulation at the transcriptional level may be involved. We would like to investigate the upstream regulatory mechanisms of the BCL-2 gene by laylin in future studies.

On the second point, we observed that laylin-KD suppressed FCCP-induced reduction in ΔΨm. Additionally, we found that laylin-KD significantly increased the protein levels of BCL-2. BCL-2 on the mitochondrial outer membrane has been reported to directly inhibit mPTP function and/or BAX/BAK pore formation by binding to BAX [17, 20, 23]. BCL-2 has been also reported to prevent FCCP-induced apoptosis by protecting mitochondorial membranes against depolarization [31]. It has been reported that FCCP-induced depolarization can lead to the fragmentation of mitochondorial membranes [31]. Consequently, BCL-2 might protect the mitochondorial membranes from fragmentation not only by suppressing mPTP and BAX/BAK pores formation but also by counteracting depolarization itself. In this study, effects of laylin on mPTP opening were not investigated. We would like to investigate effects of laylin on mPTP opening and if involved, the detailed molecular mechanisms in the future.

Regarding the third point, we found that laylin-KD suppressed STS-induced cell membrane-bound Annexin V, caspase cascade activation, and DNA fragmentation. The influx of Ca^{2+} into mitochondria induced by the treatment with STS is known to promote the opening of mPTP and induce mitochondorial membrane fragmentation due to the reduction in ΔΨm [32, 33]. Therefore, laylin-KD might suppress apoptosis by decreasing mitochondrial membrane permeability through the up-regulation of BCL-2, as discussed in the second point. On the other hand, it has been recently reported that mPTP can open without mitochondrial depolarization [34]. Taking this fact into account, we consider that further investigation on this point is necessary in the future.

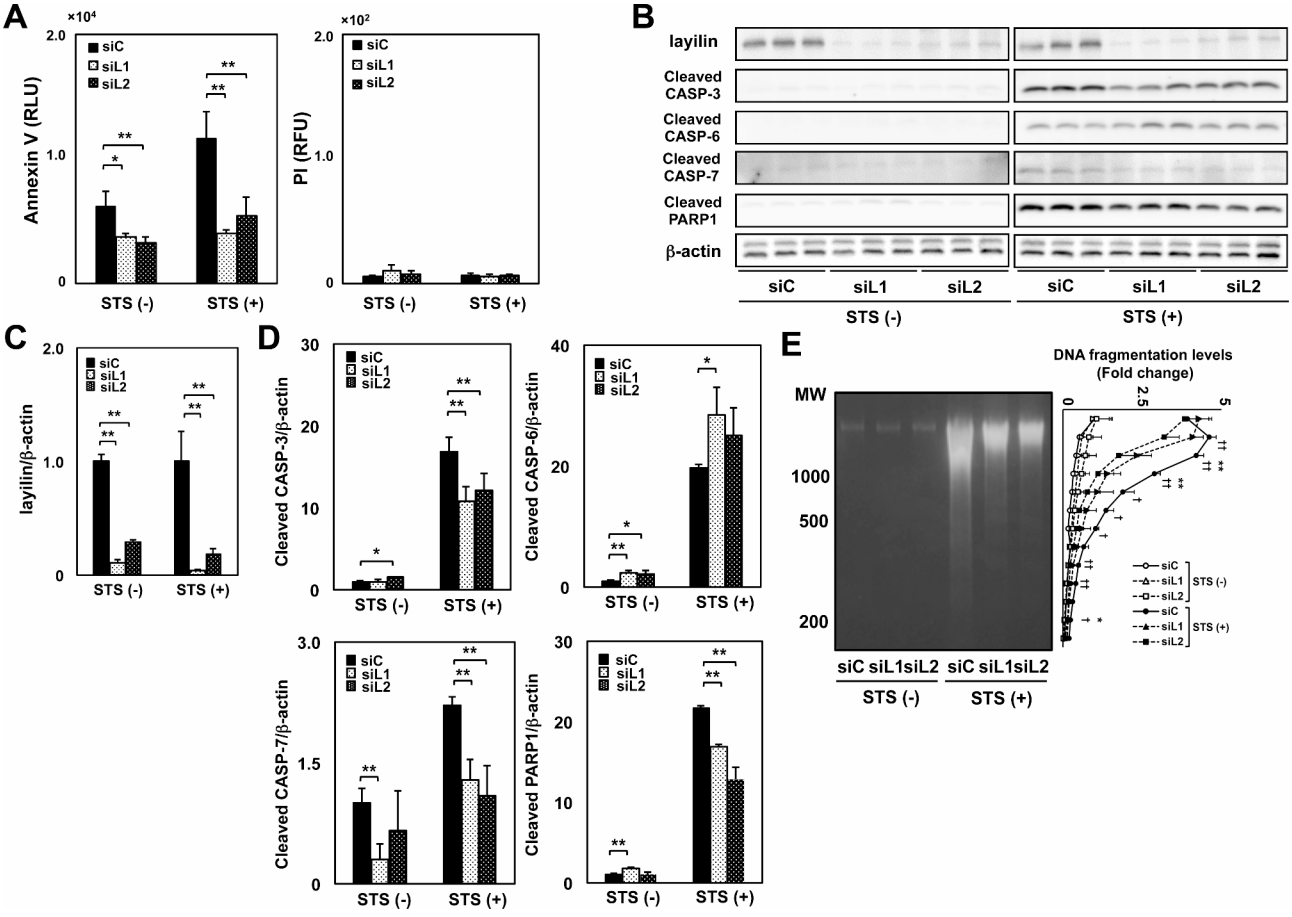

Fig. 4 Effects of layilin-KD on apoptosis-related proteins and DNA fragmentation. A172 cells were transfected with control siRNA (siC) and 2 kinds of layilin siRNA (siL1 and siL2). After 24 h, the culture medium was replaced with RPMI containing 50 μM STS. **(A)** Three hours later, cells were subjected to Annexin V and PI assay. The intensity of cell membrane-bound Annexin V and DNA-bound PI were expressed in RLU (relative luminescence units) and RFU (relative fluorescence units), respectively. **(B)** Four hours later, the protein samples extracted from the whole cells were subjected to western blotting. (**C** and **D**) Intensity of detected bands was measured by densitometry. The measured intensity of the layilin, cleaved CASP-3, cleaved CASP-6, cleaved CASP-7, and cleaved PARP1 bands was normalized using that of β-actin bands. The average of the normalized intensity of the layilin, cleaved CASP-3, cleaved CASP-6, cleaved CASP-7, and cleaved PARP1 bands in the 'siC, STS (-)' samples was defined as 1.0. Mean values with SD are presented. * $p < 0.05$, ** $p < 0.01$. **(E)** A172 cells, transfected with siL-1, siL-2 or siC (1.0×10^6 cells) in RPMI containing 10% FBS, were plated on Φ100 mm dishes. The cells were cultured with RPMI containing 400 μM STS for 4 h. Then, fragmented DNA isolated from the cells was subjected to agarose gel electrophoresis (left). DNA in the gels was visualized under ultraviolet light after staining with ethidium bromide and photographed. The intensity of the detected DNA bands was measured by densitometry. The average of the DNA fragmentation levels in the 'siC, STS (-)' samples was defined as 1.0 ($n = 3$ in each condition). Mean values with SD are shown. * $p < 0.05$, ** $p < 0.01$ (siC vs. siL1, closed), † $p < 0.05$, †† $p < 0.01$ (siC vs. siL2, closed)

Our present data suggest that layilin contributes to apoptosis by up-regulating of BAD and down-regulating of BCL-2. On the other hand, we previously reported that layilin induced metastasis-associated protein 3/snail family transcriptional repressor 1 (SNAI1)-mediated epithelial mesenchymal transition (EMT)-like change in glioblastoma cell lines such as A172 cells, enhancing their invasive ability [9]. Consequently, layilin appears to play dual roles in promoting EMT and apoptosis. Similar phenomena have been reported for tumor necrosis factor-α (TNF-α). Specifically, TNF-α has been reported to induce EMT through the transcriptional activation and protein stabilization of SNAI1 in MCF-7 cells, a human breast cancer cell line [35, 36]. On the other hand, TNF-α is well known to promote apoptosis in various cell types, including MCF-7 cells [37–39]. This suggests that certain proteins likely possess dual functions in both EMT and apoptosis. However, the factors that determine whether layilin promotes EMT or apoptosis remain unclear and warrant further investigation.

Present data suggest that layilin contributes to apoptosis in malignant glioma cells. Given that glioma cells are characterized by hyperproliferation and resistance to apoptosis, the induction of apoptosis represents a promising therapeutic strategy. Layilin can serve as a key therapeutic target in the treatment of malignant gliomas.

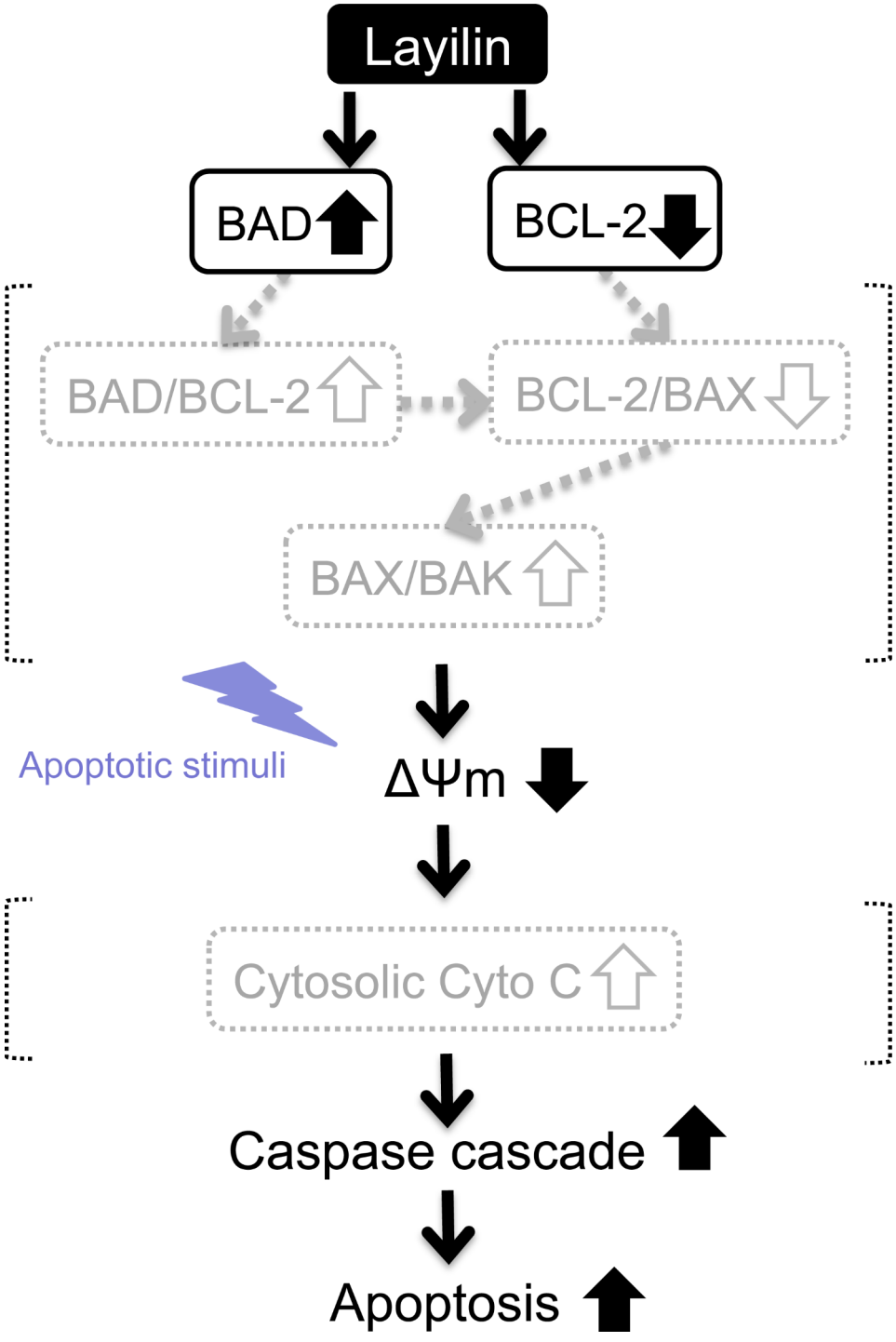

Fig. 5 Model derived from the results of this study. The results obtained in this study are shown in black text and solid lines. The parts supporting the explanation in the Discussion are shown in gray text and dashed lines, enclosed in parentheses

Conclusion

In this study, we have demonstrated that layilin plays a role in reducing ΔΨm, thereby promoting apoptosis through the up-regulation of BAD and the down-regulation of BCL-2. This research uncovers a novel function of layilin, specifically its involvement in the regulation of mitochondria-mediated apoptosis.

Abbreviations

BAD	BCL-2 associated agonist of cell death
BAK	BCL-2 antagonist/killer 1
BAX	BCL-2 associated X

BCL-2/X_L	B cell lymphoma-2/X_L
BIM	BCL-2 interacting mediator of cell death
CASP-3/6/7/9	Caspase-3/6/7/9
ΔΨm	mitochondrial membrane potential
EMT	Epithelial mesenchymal transition
FBS	Fetal bovine serum
FCCP	p-trifluoromethoxyphenylhydrazone
GAPDH	Glyceraldehyde 3-phosphate dehydrogenase
HBSS	Hanks' balanced salt solution
HRP	Horseradish peroxidase
KD	Knockdown
mPTP	mitochondrial permeability transition pore
PARP1	Poly (ADP-ribose) polymerase-1
PBS	Phosphate buffered saline
PI	Propidium idodide
RFU	Relative fluorescence units
RLU	Relative luminescence units
SNAI1	Snail family transcriptional repressor 1
STS	Staurosporine
TNF	Tumor necrosis factor

Supplementary Information

The online version contains supplementary material available at https://doi.org/10.1186/s12860-024-00521-9.

Additional file 1 Raw data (uncropped western blots) for Fig. 2A.

Additional file 2 Effects of laylin-KD on the levels of BCL-2 family proteins in U251MG cells. A similar experiment to Fig. 2 was conducted using U251MG cells.

Additional file 3 Raw data (uncropped western blots) for Additional file 2.

Additional file 4 Raw data (uncropped western blots) for Fig. 4B.

Acknowledgements

We thank Ms. Yuka Sawada and Michiyo Yokoyama for their technical assistance. This study was partly supported by JSPS KAKENHI Grant Number 22K08555 to TK and St. Marianna University School of Medicine Grant to Promote Diversity in Research Grant Number SMUGDIVR20211 to MA.

Author contributions

MA and TK conceived and supervised the study; MA, TK, and AT designed experiments; MA, AT, KO, MS and YM performed experiments; MA, TS, NS and MSK analyzed data; AT prepared Fig. 1; MA, KO, MS, TS and NS prepared Figs. 2 and 4, and 5; MA, AT, YM, and MSK prepared Fig. 3; MA, AT and TK wrote the manuscript; All authors have confirmed the contents of our manuscript.

Funding

This study was partly supported by JSPS KAKENHI Grant Number 22K08555 to TK and St. Marianna University School of Medicine Grant to Promote Diversity in Research Grant Number SMUGDIVR20211 to MA.

Data availability

The data are available from the corresponding author upon reasonable request.

Declarations

Ethics approval and consent to participate

Not applicable.

Consent for publication

Not applicable.

Competing interests

The authors declare no competing interests.

Author details

[1]Clinical Proteomics and Molecular Medicine, St. Marianna University Graduate School of Medicine, 2-16-1 Sugao, Miyamae, Kawasaki, Kanagawa 216-8511, Japan
[2]Disease Biomarker Analysis and Molecular Regulation, St. Marianna University Graduate School of Medicine, 2-16-1 Sugao, Miyamae, Kawasaki, Kanagawa 216-8511, Japan

Received: 27 February 2024 / Accepted: 11 October 2024
Published online: 25 October 2024

References

1. Goodenberger ML, Jenkins RB. Genetics of adult glioma. Cancer Genet. 2012;205:613–21. https://doi.org/10.1016/j.cancergen.2012.10.009.
2. Louis DN, Ohgaki H, Wiestler OD, et al. The 2007 WHO classification of tumours of the central nervous system. Acta Neuropathol. 2007;114:97–109. https://doi.org/10.1007/s00401-007-0243-4.
3. Louis DN, Perry A, Reifenberger G, et al. The 2016 world health organization classification of tumors of the central nervous system: a summary. Acta Neuropathol. 2016;131:803–20. https://doi.org/10.1007/s00401-016-1545-1.
4. Salvucci M, Zakaria Z, Carberry S, et al. System-based approaches as prognostic tools for glioblastoma. BMC Cancer. 2019;19:1092. https://doi.org/10.1186/s12885-019-6280-2.
5. Borowsky ML, Hynes RO. Layilin, a novel talin-binding transmembrane protein homologous with C-type lectins, is localized in membrane ruffles. J Cell Biol. 1998;143:429–42. https://doi.org/10.1083/jcb.143.2.429.
6. Bono P, Rubin K, Higgins JM, et al. Layilin, a novel integral membrane protein, is a hyaluronan receptor. Mol Biol Cell. 2001;12:891–900. https://doi.org/10.1091/mbc.12.4.891.
7. Bono P, Cordero E, Johnson K, et al. Layilin, a cell surface hyaluronan receptor, interacts with merlin and radixin. Exp Cell Res. 2005;308:177–87. https://doi.org/10.1016/j.yexcr.2005.04.017.
8. Zheng C, Zheng L, Yoo JK, et al. Landscape of infiltrating T cells in Liver Cancer revealed by single-cell sequencing. Cell. 2017;169:1342–56. https://doi.org/10.1016/j.cell.2017.05.035.
9. Kaji T, Arito M, Tsutiya A, et al. Layilin enhances the invasive ability of malignant glioma cells via SNAI1 signaling. Brain Res. 2019;1719:140–7. https://doi.org/10.1016/j.brainres.2019.05.034.
10. Tsutiya A, Arito M, Tagashira T, et al. Layilin promotes mitochondrial fission by cyclin-dependent kinase 1 and dynamin-related protein 1 activation in HEK293T cells. Biochem Biophys Res Commun. 2021;549:143–9. https://doi.org/10.1016/j.bbrc.2021.02.091.
11. Hajnóczky G, Davies E, Madesh M, et al. Calcium signaling and apoptosis. Biochem Biophys Res Commun. 2003;304:445–54. https://doi.org/10.1016/S0006-291X(03)00616-8.
12. Bauer TM, Murphy E. Role of mitochondrial calcium and the permeability transition pore in regulating cell death. Circul Res. 2020;126:280–93. https://doi.org/10.1161/CIRCRESAHA.119.316306.
13. Lemasters JJ, Theruvath TP, Zhong Z, et al. Mitochondrial calcium and the permeability transition in cell death. Biochim Biophys Acta. 2009;1787:1395–401. https://doi.org/10.1016/j.bbabio.2009.06.009.
14. Karbowski M, Youle RJ. Dynamics of mitochondrial morphology in healthy cells and during apoptosis. Cell Death Differ. 2003;10:870–80. https://doi.org/10.1038/sj.cdd.4401260.
15. Valdebenito GE, Duchen MR. Monitoring mitochondrial membrane potential in live cells using time-lapse fluorescence imaging. In: Tomar, N, editors Mitochondria. Methods Mol Biol. 2022;2497. https://doi.org/10.1007/978-1-0716-2309-1_22
16. Gross A, McDonnell JM, Korsmeyer SJ. BCL-2 family members and the mitochondria in apoptosis Genes dev. 1999;13:1899–911. https://doi.org/10.1101/gad.13.15.1899.
17. Singh R, Letai A, Sarosiek K. Regulation of apoptosis in health and disease: the balancing act of BCL-2 family proteins. Nat Rev Mol Cell Biol. 2019;20:175–93. https://doi.org/10.1038/s41580-018-0089-8.
18. Mikhailov V, Mikhailova M, Degenhardt K, et al. Association of Bax and bak homo-oligomers in mitochondria. Bax requirement for bak reorganization and cytochrome c release. J Biol Chem. 2003;278:5367–76. https://doi.org/10.1074/jbc.M203392200.

19. Peña-Blanco A, García-Sáez AJ. Bax, Bak and beyond_Mitochondrial performance in apoptosis. FEBS J. 2018;285:416–31. https://doi.org/10.1111/febs.14186.
20. Whelan RS, Konstantinidis K, Wei AC et al. Bax regulates primary necrosis through mitochondrial dynamics. Proc Natl Acad Sci U S A 2012;109:6566–571. https://doi.org/10.1073/pnas.1201608109.
21. Hengartner M. The biochemistry of apoptosis. Nature. 2000;407:770–6. https://doi.org/10.1038/35037710.
22. Slee EA, Harte MT, Kluck RM, et al. Ordering the cytochrome c-initiated caspase cascade: hierarchical activation of caspases-2, -3, -6, -7, -8, and – 10 in a caspase-9-dependent manner. J Cell Biol. 1999;144:281–92. https://doi.org/10.1083/jcb.144.2.281.
23. Tsujimoto Y. Role of Bcl-2 family proteins in apoptosis: apoptosomes or mitochondria? Genes Cells. 1998;3:697–707. https://doi.org/10.1046/j.1365-2443.1998.00223.x.
24. Oltvai ZN, Milliman CL, Korsmeyer SJ. Bcl-2 heterodimerizes in vivo with a conserved homolog, Bax, that accelerates programmed cell death. Comp Study Cell. 1993;74:609-19. https://doi.org/10.1016/0092-8674(93)90509-o.
25. Hirotani M, Zhang Y, Fujita N, et al. NH2-terminal BH4 domain of Bcl-2 is functional for heterodimerization with Bax and inhibition of apoptosis. J Biol Chem. 1999;274:20415–20. https://doi.org/10.1074/jbc.274.29.20415.
26. Schindelin J, Arganda-Carreras I, Frise E, et al. Fiji: an open-source platform for biological-image analysis. Nat Methods. 2012;9:676e682. https://doi.org/10.1038/nmeth.2019.
27. Asano K, Arito M, Kurokawa MS, et al. Secretion of inflammatory factors from chondrocytes by layilin signaling. Biochem Biophys Res Commun. 2014;452:85–90. https://doi.org/10.1016/j.bbrc.2014.08.053.
28. Sakai Y, Taguchi M, Morikawa Y, et al. Apoptotic mechanism in human brain microvascular endothelial cells triggered by 40-iodo-α-pyrrolidinononanophenone: contribution of decrease in antioxidant properties. Toxicol Lett. 2022;355:127–40. https://doi.org/10.1016/j.toxlet.2021.11.018.
29. Suyama K, Sakai D, Hayashi S, et al. Bag-1 protects Nucleus Pulposus cells from oxidative stress by interacting with HSP70. Biomedicines. 2023;11:863. https://doi.org/10.3390/biomedicines11030863.
30. Yang E, Zha J, Jockel J, et al. Bad, a heterodimeric partner for Bcl-XL and Bcl-2, displaces Bax and promotes cell death. Cell. 1995;80:285–91. https://doi.org/10.1016/0092-8674(95)90411-5.
31. Dispersyn G, Nuydens R, Connors R, et al. Bcl-2 protects against FCCP-induced apoptosis and mitochondrial membrane potential depolarization in PC12 cells. Biochim Biophys Acta. 1999;1428(2–3):357–71. https://doi.org/10.1016/s0304-4165(99)00073-2.
32. Prudent J, Zunino R, Sugiura A. MAPL SUMOylation of Drp1 stabilizes an ER/Mitochondrial platform required for cell death. Mol Cell. 2015;59:941–55. https://doi.org/10.1016/j.molcel.2015.08.001.
33. Hurst S, Hoek J, Sheu SS. Mitochondrial Ca^{2+} and regulation of the permeability transition pore. J Bioenerg Biomembr. 2016;49:27–47. https://doi.org/10.1007/s10863-016-9672-x.
34. Neginskaya MA, Morris SE, Pavlov.Both EV. ANT and ATPase are essential for mitochondrial permeability transition but not depolarization. iScience. 2022;25:105447. https://doi.org/10.1016/j.isci.2022.105447.
35. Dong R, Wang Q, He XL, et al. Role of nuclear factor kappa B and reactive oxygen species in the tumor necrosis factor-alpha-induced epithelial-mesenchymal transition of MCF-7 cells. Braz J Med Biol Res. 2007;40:1071–8. https://doi.org/10.1590/s0100-879x2007000800007.
36. Wu Y, Deng J, Rychahou PG, et al. Stabilization of snail by NF-kappaB is required for inflammation-induced cell migration and invasion. Cancer Cell. 2009;15:416–28. https://doi.org/10.1016/j.ccr.2009.03.016.
37. Jiang Y, Porter AG. Prevention of tumor necrosis factor (TNF)-mediated induction of p21WAF1/CIP1 sensitizes MCF-7 carcinoma cells to TNF-induced apoptosis. Biochem Biophys Res Commun. 1998;245:691–7. https://doi.org/10.1006/bbrc.1998.8390.
38. Rozen F, Zhang J, Pollak M. Antiproliferative action of tumor necrosis factor-alpha on MCF-7 breast cancer cells is associated with increased insulin-like growth factor binding protein-3 accumulation. Int J Oncol. 1998;13:865–9. https://doi.org/10.3892/ijo.13.4.865.
39. Burow ME, Weldon CB, Melnik LI, et al. PI3-K/AKT regulation of NF-kappaB signaling events in suppression of TNF-induced apoptosis. Biochem Biophys Res Commun. 2000;271:342–5. https://doi.org/10.1006/bbrc.2000.2626.

Publisher's note